MITSUBISHI ELECTRIC RESEARCH LABORATORIES
https://www.merl.com

A Physics-Constrained Data-Driven Modeling Approach for Vapor Compression Systems

Ma, JiaCheng; Qiao, Hongtao; Laughman, Christopher R.

TR2024-102 July 26, 2024

Abstract

Data-driven dynamic models typically offer faster execution than their physics-based counterparts described by large systems of nonlinear and stiff differential-algebraic equations with satisfactory accuracy. Therefore, development of accurate but computationally efficient models directly identified from data constitutes a solution path for investigating controls, fault detection and diagnostics of vapor compression systems (VCS). A modular approach of generating and interconnecting data-driven component models enables reuse of readily trained models and adaption to arbitrary system configurations. Despite the flexibility, a modular integration for system model generation can suffer from nonphysical behaviors of violating conservation laws due to inevitable prediction errors associated with each component model. This paper presents a data-driven dynamic modeling approach for VCS that exploits state-of-the-art deep learning methods for constructing component models while enforcing physical conservation for system simulations. Specifically, gated recurrent unit (GRU) and feedforward neural network models are employed for heat exchangers and mass-flow devices. Predictive capabilities and conservation properties of the proposed modeling approach is demonstrated via a case study of an air-source heat pump system. Simulation results reveal a significant speedup with negligible discrepancies compared to high-fidelity physics-based models.

International Refrigeration and Air Conditioning Conference at Purdue 2024

Mitsubishi Electric Research Laboratories, Inc.
201 Broadway, Cambridge, Massachusetts 02139

A Physics-Constrained Data-Driven Modeling Approach for Vapor Compression Systems

Jiacheng Ma[1], Hongtao Qiao[2*], Christopher R. Laughman[2]

[1] Ray W. Herrick Laboratories, School of Mechanical Engineering, Purdue University,
West Lafayette, IN, USA
ma516@purdue.edu

[2] Mitsubishi Electric Research Laboratories,
Cambridge, MA, USA
qiao@merl.com, laughman@merl.com

* Corresponding Author

ABSTRACT

Data-driven dynamic models typically offer faster execution than their physics-based counterparts described by large systems of nonlinear and stiff differential-algebraic equations with satisfactory accuracy. Therefore, development of accurate but computationally efficient models directly identified from data constitutes a solution path for investigating controls, fault detection and diagnostics of vapor compression systems (VCS). A modular approach of generating and interconnecting data-driven component models enables reuse of readily trained models and adaption to arbitrary system configurations. Despite the flexibility, a modular integration for system model generation can suffer from nonphysical behaviors of violating conservation laws due to inevitable prediction errors associated with each component model. This paper presents a data-driven dynamic modeling approach for VCS that exploits state-of-the-art deep learning methods for constructing component models while enforcing physical conservation for system simulations. Specifically, gated recurrent unit (GRU) and feedforward neural network models are employed for heat exchangers and mass-flow devices. Predictive capabilities and conservation properties of the proposed modeling approach is demonstrated via a case study of an air-source heat pump system. Simulation results reveal a significant speedup with negligible discrepancies compared to high-fidelity physics-based models.

1. INTRODUCTION

Development of accurate and computationally affordable dynamic models serves an important role in design and operation of vapor compression systems (VCS) by facilitating system performance analysis, design and evaluation of control, fault detection and diagnostics (FDD) algorithms, etc. Despite a great amount of research efforts in dynamic VCS modeling over past decades, there exists room for further advancements in modeling approaches concerning simulation accuracy, efficiency and robustness. The most commonly seen modeling paradigm appearing in the literature falls under the category of gray-box models, which are largely built upon physical conservation laws but incorporate empirical correlations with available data to simplify certain descriptions such as performance maps for mass-flow devices and heat transfer correlations (Rasmussen, 2012). In the following context, these models are referred to as physics-based models, in order to draw a distinction from black-box or data-driven models. To capture the complicated thermo-fluid behaviors of VCS, physics-based models are described by a set of governing conservation equations, i.e., mass, energy, and momentum. A solution scheme for these models generally involves spatial discretization and nonlinear algebraic coupling (Laughman & Qiao, 2018), which results in large systems of nonlinear differential algebraic equations (DAEs). Consequently, the applicability of physics-based dynamic models for design, control and FDD purposes continues to encounter remarkable challenges including computational costs and numerical robustness, as the complexity and scale of system configurations tend to increase rapidly in the near future (Goyal et al., 2019; Ma et al., 2021).

Data-driven dynamic models constitute a solution path regarding challenges for real-time applications, as they omit vastly the underlying physics of the phenomena within components. With advances in data-driven modeling techniques and enrichment of large-scale experimental data sets, these models have been investigated for steady-state performance

prediction of VCS and their components, e.g. (Shao et al., 2012). However, a very limited number of studies have focused on characterizing the nonlinear dynamic behaviors. Among them, it appears to be a common treatment to develop a single data-driven model for capturing the dynamics of an entire system, neglecting individual and interconnection behaviors of components (Habtom, 1999; Yoon & Lee, 2010; Chen & Fu, 2020). As a consequence, a model generated in this manner is solely valid for a specific system of interest, without any ease in modifying system configurations. Furthermore, training of a system-level model can be prohibitively expensive for large-scale system architectures such as variable refrigerant flow (VRF) applications.

A modular implementation is therefore attractive for general-purpose model development. Creating and integrating data-driven or a combination of data-driven and physics-based component models offers the flexibility to reuse readily trained models for arbitrary cycle configurations. In this context, Chen et al. (2022) explored the paradigm of integrating data-driven component models that were constructed using deep learning techniques into a system model for a vehicle air conditioner. However, the surveyed approach is not sufficiently generic since component models are implicitly coupled at the training stage. Moreover, conservation properties (e.g., mass and energy conservation) of the data-driven models were not examined in previous efforts, as it is identified as a fundamental challenge in data-driven modeling to satisfy physical conservation (Hansen et al., 2023).

Clearly a literature screening indicates an absence of a general modeling framework for VCS that can incorporate physics-constrained data-driven modeling techniques for constructing component models and consequently system models for arbitrary configurations. This paper exploited state-of-the-art deep learning techniques for constructing component models of VCS. Generalized model interfaces and solution schemes were proposed for dynamic and quasi-steady-state components to enforce physical conservation when integrating data-driven component models to complete a system model. Performance of the proposed modeling approach was demonstrated using a case study of an air-source heat pump (ASHP) and comparisons against high-fidelity physics-based models implemented in Modelica. In summary, the proposed data-driven modeling framework aims to address the following issues

- Modular model implementation: data-driven component models are generated individually and integrated into system models to enable model reuse and flexible adaption to arbitrary system configurations.
- Physical conservation enforcement: The design of fast, accurate and robust data-driven component models involves superimposing constraints of physical conservation laws that lead to physically conserving system model aggregation.

The remainder of this paper is structured as follows. Section 2 describes methodologies of component modeling and system model integration. Section 3 presents a case study where data-driven models are generated for an ASHP system and compared with physics-based Modelica models to demonstrate the efficacy of the proposed approach. Section 4 summarizes conclusions of the present paper.

2. METHODOLOGIES

The modularity of data-driven dynamic vapor compression system (VCS) modeling can be realized by constructing models that capture the behavior of each individual component and then integrating them following the physical conservation laws. Since the dominant dynamics reside in two-phase heat exchangers (HX), autoregressive time-series prediction modeling approaches can be employed to capture the complex behavior, while mass-flow devices such as compressors and valves are effectively modeled using feedforward formulations with nonlinear function mappings under quasi-steady-state assumptions.

2.1 Mass-flow device models: feedforward neural networks

Development of quasi-steady-state component models for mass-flow devices is generally carried out as a multi-input-multi-output (MIMO) mapping task. In the present work, feedforward neural networks are employed to construct compressor and expansion valve models.

Variable-speed compressor models generally take inputs of the refrigerant suction state, discharge pressure and actuation signals, while predicting mass flow rate, power and discharge temperature or enthalpy as outputs. Black-box models (e.g., 10-coefficient polynomials) rely on a large set of data for training and usually suffer from non-physical behaviors and poor extrapolation performance outside the operating envelope that is specified to generate the data. Therefore, instead of direct input-output mapping, physical knowledge can be incorporated by mapping from inputs to efficiencies that describe compression processes (Yang et al., 2009) along with conservation laws. Consequently,

feedforward neural networks are exploited to define a mapping $\mathbf{y} = \mathbf{f}(\mathbf{x})$ with

$$\mathbf{y} = \begin{bmatrix} \eta_v & \eta_{is} & f_{loss} \end{bmatrix}^T \in \mathbb{R}^3, \tag{1}$$

$$\mathbf{x} = \begin{bmatrix} \omega & p_{suc} & h_{suc} & p_{dis} \end{bmatrix}^T \in \mathbb{R}^4 \tag{2}$$

where outputs consist of volumetric efficiency η_v, isentropic efficiency η_{is} and heat loss factor f_{loss}, while model inputs are compressor speed, suction pressure, suction enthalpy and discharge pressure. After that, compressor performance can be predicted utilizing those neural network model outputs and readily available inputs. The refrigerant mass flow rate is calculated by

$$\dot{m} = \omega \eta_v \rho_{suc} V_s \tag{3}$$

where V_s is the displacement of compressor volume and ρ_{suc} is the suction density retrieved from the suction state. The power consumption is determined by

$$P = \frac{\dot{m}(h_{dis,is} - h_{suc})}{\eta_{is}} \tag{4}$$

where $h_{dis,is}$ is the discharge enthalpy assuming an isentropic compression process. Afterwards, the discharge enthalpy can be obtained by formulating an energy balance across the compressor

$$h_{dis} = h_{suc} + \frac{P - \dot{Q}_{loss}}{\dot{m}} \tag{5}$$

where the heat loss is obtained as a ratio to the power input using the predicted heat loss factor $\dot{Q}_{loss} = f_{loss} P$. It is important to note that by predicting these dimensionless efficiencies using neural network models, the overall compressor model is applicable to other refrigerants since thermodynamic property evaluations are absent during training given a dataset of inputs and outputs specified in Eq. (1) and (2). In addition, compressor model outputs can be bounded to physically feasible values by limiting predicted efficiencies to valid ranges, which is essential to robust system simulations when coupled to other component models.

Expansion valve modeling follows a similar fashion as the compressor. A feedforward neural network is trained to predict a combined term of discharge coefficient C_d and valve opening area A that is usually unavailable to model development with model inputs of inlet pressure, inlet enthalpy, outlet pressure as well as a normalized valve opening $\varphi \in [0, 1]$. The refrigerant mass flow rate through the valve can subsequently be predicted by adopting a typical throttling process description

$$\dot{m} = C_d A \sqrt{2 \rho_{in} (p_{in} - p_{out})}. \tag{6}$$

Furthermore, the expansion process is assumed to be enthalpic which leads to $h_{out} = h_{in}$. To summarize, a mapping for expansion valve models is specified as

$$\mathbf{y} = \begin{bmatrix} C_d A & h_{out} \end{bmatrix}^T \in \mathbb{R}^2 \tag{7}$$

$$\mathbf{x} = \begin{bmatrix} p_{in} & h_{in} & p_{out} & \varphi \end{bmatrix}^T \in \mathbb{R}^4. \tag{8}$$

Figure 1 outlines feedforward neural networks employed in the present work for compressor and expansion valve modeling.

2.2 Two-phase heat exchanger modeling: gated recurrent unit

Without access to internal states that characterize heat exchanger (HX) dynamics, data-driven models seek a nonlinear approximator $\mathbf{f}(\cdot)$ that can predict observable outputs $\mathbf{y}_t$ at time instance t depending on historical values of inputs and outputs to certain orders

$$\mathbf{y}_t = \mathbf{f}(\mathbf{y}_{t-n_y:t-1}, \mathbf{u}_{t-n_u:t}) \tag{9}$$

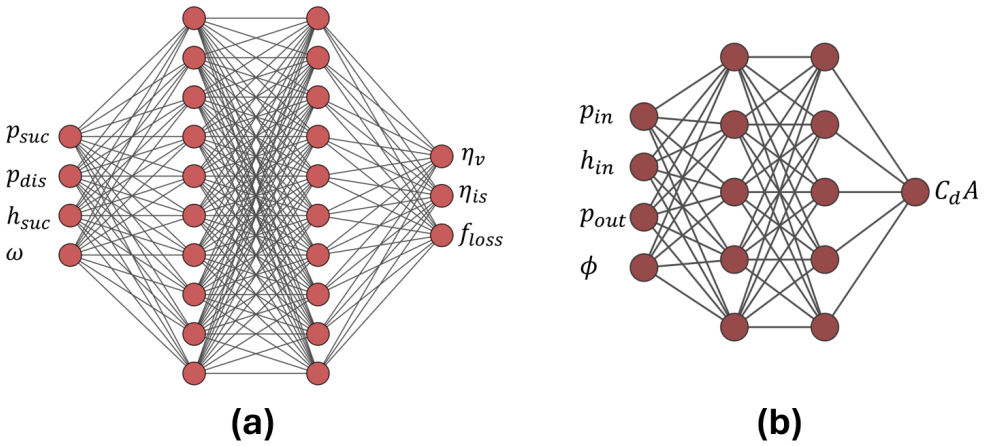

Figure 1: Data-driven mass-flow device models using feedforward neural networks: (a) compressor; (b) expansion valve.

where a time interval of 1 second is utilized here and in the following context for illustration.

Apparently, the selection of look-back window lengths n_y and n_u is of critical importance to the performance of resulting models, as a trade-off between prediction accuracy and model complexities. Apart from that, choices of input and output variables play a vital role in model prediction capabilities. Regarding a HX as a generic control volume, input-output responses are typically captured by the time evolution of the refrigerant and the secondary fluid states at the inlet and outlet of each flow path. Figure 2 depicts those variables for a fin-and-tube HX commonly employed in an ASHP system, where inlet mass flow rate and enthalpy, back pressure, and upstream enthalpy at the outlet in a reverse-flow scenario are featured as inputs for the refrigerant flow, while inlet conditions, flow rate and ambient pressure are considered for the air side. Correspondingly, outputs of a HX model include the refrigerant states at infinitesimal points on edges of the HX inlet and exit as well as exit temperature and heat capacities of the air flow.

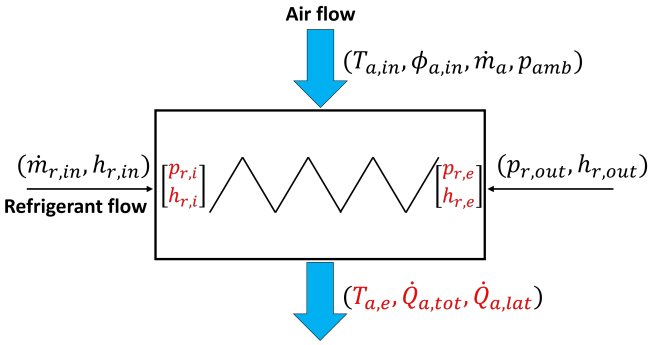

Figure 2: Overview of input and output variables commonly adopted for data-driven HX modeling that may violate conservation laws (output variables are marked in red).

This setup seems adequate at first glance concerning the predictive performance of a HX component model, however, issues of violating conservation laws arise when such models are integrated into a system. Consider an ASHP system comprised of n HXs and m mass-flow devices. An energy balance can be formed with regard to the entire system as

$$\frac{dE_{sys}}{dt} = \sum_{k=1}^{n} \dot{Q}_k + \sum_{k=1}^{m} (P_k - \dot{Q}_{k,loss}) \tag{10}$$

where E_{sys} represents the internal energy of the entire system, $\dot{Q}_k$ represents the air-side capacity of each HX following the sign convention that inflow energy (e.g., for an evaporator) is positive and outflow is negative, P_k and $\dot{Q}_{k,loss}$ are

power input and heat loss of each mass-flow device, respectively. Since capacities, power and heat loss are predicted separately by individual component models, their balance can not be enforced at steady-state conditions due to inevitable prediction errors, consequently violating the energy conservation stated in Eq. (10). To tackle this issue, the internal energy of a HX is incorporated as a model input and updated subject to a forward difference scheme with a time step Δt

$$E_{k,t+1} = E_{k,t} + (\dot{m}_{k,in}h_{k,in} - \dot{m}_{k,out}h_{k,out} + \dot{Q}_k)\Delta t \quad k = 1, 2, \ldots, n \tag{11}$$

which describes the heat exchanger energy balance in a discrete-time form. Usually air-side mass and energy storage is negligible for cross-flow coil configurations, which leads to a quasi-steady-state model description. As a result, HX internal energy is composed of energy storage in the refrigerant and metal walls. Following this scheme, the total energy source for a system at every time step can be obtained by summing up those of heat exchangers as shown in Eq. (11), since mass flow devices are modeled as static components without energy storage

$$\Delta E_{tot} = \sum_{k=1}^{n} (\dot{m}_{k,in}h_{k,in} - \dot{m}_{k,out}h_{k,out} + \dot{Q}_k). \tag{12}$$

Along the refrigerant loop, enthalpy flows across mass flow devices can be represented equivalently using power and heat loss of those components according to the energy balance as revealed in Eq. (5), while intermediate quantities in between heat exchangers are canceled out. As a consequence, the total energy source obtained from HX models corresponds to that for the entire system appearing in Eq. (10), which indicates that under the current setup system energy conservation is respected at steady-state conditions as HX models evolve to $E_{k,t+1} = E_{k,t}$.

A similar argument can be made for system mass conservation. Of equal importance to realize system energy balance is to ensure a consistent refrigerant charge prediction for the overall system. It can be easily understood that predicting the refrigerant charge residing in a HX as a model output leads to an inconsistent total charge prediction over time due to inevitable prediction errors associated with each HX model. Therefore, the refrigerant charge is considered as an input to a HX model and is updated according to a discrete-time mass balance (Dong et al., 2024)

$$M_{k,t+1} = M_{k,t} + (\dot{m}_{k,in} - \dot{m}_{k,out})\Delta t \tag{13}$$

which reveals that the total refrigerant charge across the system remains constant $\sum_{k=1}^{n} M_{k,t+1} = \sum_{k=1}^{n} M_{k,t}$ once models are initialized, since interface mass flow rates are canceled out at every time step.

As per the above discussion, the ultimate sets of input and output variables selected for HX model development in Eq. (9) are outlined as

$$\mathbf{u} = \begin{bmatrix} T_{a,in} & \varphi_{a,in} & \dot{m}_a & p_{amb} & \dot{m}_{r,in} & h_{r,in} & h_{r,out} & p_{r,out} & M_r & E_r \end{bmatrix}^T \in \mathbb{R}^{10}, \tag{14}$$

$$\mathbf{y} = \begin{bmatrix} p_{r,i} & h_{r,i} & p_{r,e} & h_{r,e} & T_{a,e} & \dot{Q}_{a,tot} & \dot{Q}_{a,lat} \end{bmatrix}^T \in \mathbb{R}^7. \tag{15}$$

It is essential to note that this setup is generally applicable to the development of mass and energy conserving data-driven HX models, invariant to time-series forecasting modeling techniques. This work exploits capability and efficiency of recurrent neural networks (RNN) in identifying the complicated thermo-fluid dynamics. Specifically, gated recurrent unit (GRU) as a particular RNN architecture invented to mitigate the vanishing gradient problem is considered (Rehmer & Kroll, 2019). GRU is specialized for learning long-term dependencies within sequential data among deep learning models. An encoder-decoder sequence-to-sequence GRU architecture is adopted in the present work. As shown in Figure 3, sequences of input features and outputs tracked with a look-back window of context length N are augmented as an input context sequence $\mathbf{x}_{T-N:T-1}$ to the multi-layer GRU network. An encoder GRU block processes the input sequence and then a decoder GRU block generates the predicted output sequence subject to a given length. In terms of a HX model, the output sequence length is set to one since further predictions can only be made until the cycle model is solved at the current time step. Each of the encoder and decoder blocks consists of 2 GRU layers in this work. After the hidden state if computed for the last GRU layer of the decoder, it is subsequently passed through a set of fully connected layers consisting of a linear layer, a rectified linear unit (ReLU) layer followed by another linear layer that map the hidden state to an output sequence y_T, which concludes predictions at the current time step. This procedure is then repeated by updating the context sequence with input features for the next time step $\mathbf{u}_{T+1}$ and the predicted outputs $\mathbf{y}_T$.

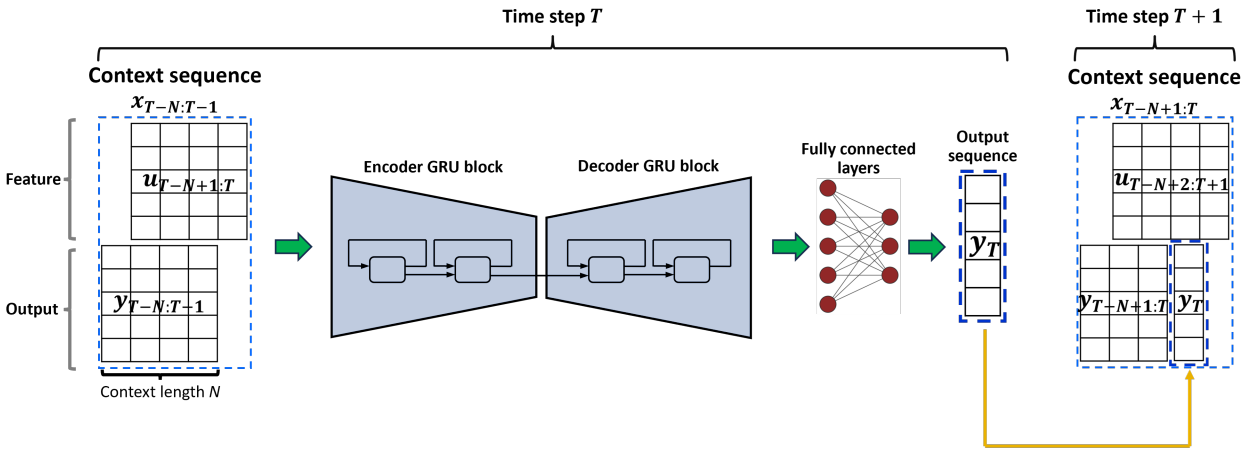

Figure 3: An illustration of the GRU architecture for HX model with one-step prediction.

Training the aforementioned model involves first processing time-series data of feature and output trajectories as context and output sequences. A sliding window of length $N+1$ is applied to the raw transient data to truncate it into shortened pieces spanning $[T-N, T]$ where $u_{T-N+1:T}$ and $y_{T-N:T-1}$ are augmented to form a context sequence and the training target y_T is used to compute the losses with model predictions. The entire dataset of transient pieces is then split into training, validation and testing sets, respectively. The mean squared error (MSE) is adopted to measure the training loss of each truncated piece, which then adds up to the total loss. After each training epoch, the loss over the validation set is evaluated to adapt the learning rate by a reduction factor when it stops decreasing for a certain number of consecutive epochs.

2.3 System solution

While each component model is characterized by a uniquely selected set of input/output variables to ensure individual model performance, a system solution scheme is necessary for modular-based dynamic modeling to orderly integrate component models and progress model predictions over time. As continuity equations are formed when interconnecting component models, the refrigerant states at junctions remain unknown at every time step and involve numerical iterations for solutions when connected components share the same boundary conditions. Specifically, the refrigerant pressure is considered a boundary condition/input at ports of mass-flow devices and the nominal exit port of HXs for data-driven models derived before. As a result, residual equations are formed to solve for interface pressures at every time step during simulations to enforce continuity. Consider the heat exchanger model setup shown in Figure 2, the refrigerant exit mass flow rate is calculated according to the difference between the predicted exit pressure and the back pressure, which relates to frictional pressure drops under the assumption of static momentum balances. In the present work, the frictional pressure drop is correlated using a power law

$$\Delta p = K\Delta p_0 \left(\frac{\dot{m}}{\dot{m}_0}\right)^{\alpha} \tag{16}$$

where Δp_0 denotes the pressure drop at a nominal condition corresponding to a mass flow rate $\dot{m}_0$, K and α are fitted coefficients to account for various operating conditions. When a HX model is coupled to a mass-flow device model, the back pressure should be iterated to satisfy the continuity constraint at each time step. This can be illustrated using a four-component cycle configuration depicted in Figure 4. Two independent residual equations are formed to solve for interface pressures

$$F\left(\begin{bmatrix} p_a \\ p_b \end{bmatrix}\right) = \begin{bmatrix} \dot{m}_1(p_a) - \dot{m}_2(p_a) \\ \dot{m}_3(p_b) - \dot{m}_4(p_b) \end{bmatrix} = \mathbf{0} \tag{17}$$

where $\dot{m}_1(\cdot)$ and $\dot{m}_3(\cdot)$ represent the static momentum balance in Eq. (16) rewritten explicitly as a function of the back pressure for obtaining mass flow rates, $\dot{m}_2(\cdot)$ and $\dot{m}_4(\cdot)$ represent the compressor and expansion valve models for determining mass flow rates as shown in Eq. (3) and (6). During online simulations, the system of residual equations in Eq.(17) can be solved by multivariate root-finding algorithms such as Powell's method (Kochenderfer & Wheeler, 2019).

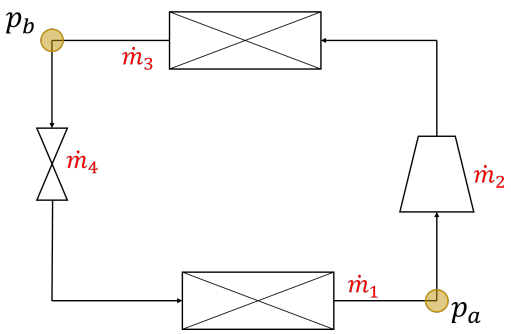

Figure 4: Interface pressures solved by iterations for a four-component cycle.

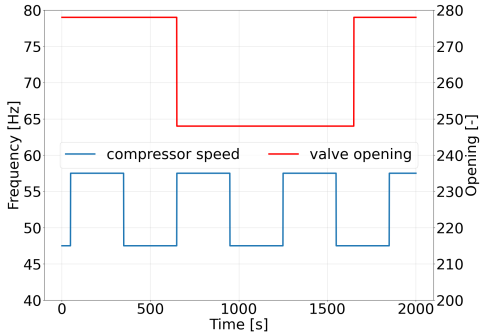

Figure 5: Compressor and valve actuation for system load-change transients.

3. CASE STUDY: AN AIR-SOURCE HEAT PUMP

3.1 Generating data-driven models

A basic ASHP system configuration comprised of fin-and-tube condenser and evaporator, a scroll compressor and an electronic expansion valve is considered for demonstration. R32 is used as the working fluid. Physics-based component models are constructed for the system using Modelica. The compressor and expansion valve models are similar to those described in Section 2 except for the fact that efficiency maps are fitted with high-order polynomials. Dynamic HX modeling is carried out using a finite volume approach for discretizing governing conservation equations. Moreover, the HX models are formulated to capture spatial variations along coil circuitry by dividing each tube into several control volumes and connecting them based on the actual multi-row coil circuitry configurations. As a consequence, a high-dimensional differential algebraic equation system is formed for a HX model. Refer to Qiao et al. (2015) for a comprehensive description of the physics-based model development. In the present study, compressor speeds and EXV opening are actuated to drive system transients in heating operations, while fan speeds and ambient conditions including inlet air temperature and humidity for each HX are fixed. The condenser (indoor coil) inlet air temperature, relative humidity, and volume flow rate are 20°C, 60%, and 0.4 m^3/s, respectively, while the evaporator air-side inputs are 7°C, 87%, and 0.72 m^3/s.

Physics-based heat exchanger models are excited by boundary condition profiles to collect trajectories of model predictions. In order to capture model behaviors both under steady-state and transient conditions, an input profile is constructed with consecutive step perturbations where the step length is selected so that the model can reach steady-state before boundary conditions are perturbed again. Concerning those on the refrigerant side, profiles of the inlet mass flow rate and enthalpy, outlet enthalpy and back pressure are generated by performing random walks within a feasible space to extensively explore the input space, aiming to improve the generalization capability of trained models. The magnitude of each step is determined by $\mathbf{u}[k+1] = \mathbf{u}[k] + \mathbf{Z}\mathcal{N}(0, \mathbf{I}_4)$ where $\mathcal{N}(0, \mathbf{I}_4)$ is a vector of standard Gaussian random numbers and $\mathbf{Z}$ is a diagonal matrix that controls magnitudes of each step change for input variables. The generated path of each input is then converted to a profile of step changes and bounded to feasible values. 500 steps of random walk are carried out and input profiles with a step length of 30s are generated to simulate condenser and evaporator models. The time-series model predictions are obtained with a sampling interval of 1 second. Trajectories of the predicted refrigerant charge and coil internal energy are augmented with input profiles to obtain the training input data as specified in Eq. (14), along with predicted output variables specified in Eq. (15) to complete the training dataset. A context length of 2 is selected for the input sequence in the present study. That means model outputs tracked back 2 seconds, features of the previous step along with those of the current step are fed into the GRU model as a context sequence to predict current output variables. The hidden size of each GRU layer is set to 256, and an initial learning rate of 2×10^{-4} is applied. Each HX model is trained for 50 epochs with a batch size of 64.

Collecting training data for static models of mass-flow devices is approached in a straightforward way by randomly generating samples in the input space without a need for random walk, since outputs of these models do not embrace time dependency. A feedforward neural network of 2 hidden layers and 10 neurons per layer is adopted for the compressor model with the sigmoid activation function. The network is trained using 10^4 samples for 1000 epochs with a batch size of 128. Training of the expansion valve model follows the same process where a network of 2 hidden

layers and 5 nodes per layer is found appropriate for valve mass flow predictions. All of the data-driven models are implemented using PyTorch with a CPU, and trained using an Adam optimizer (Kingma & Ba, 2014).

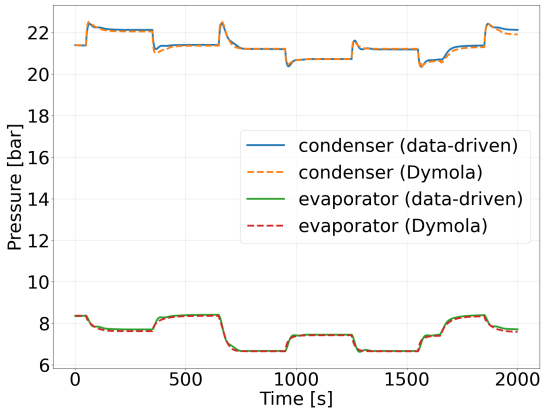

(a) Refrigerant pressures.

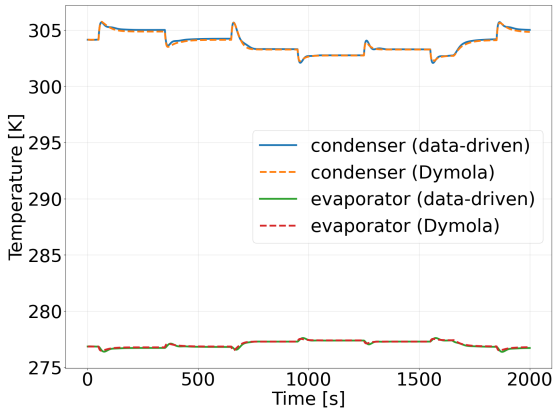

(b) Air exit temperatures.

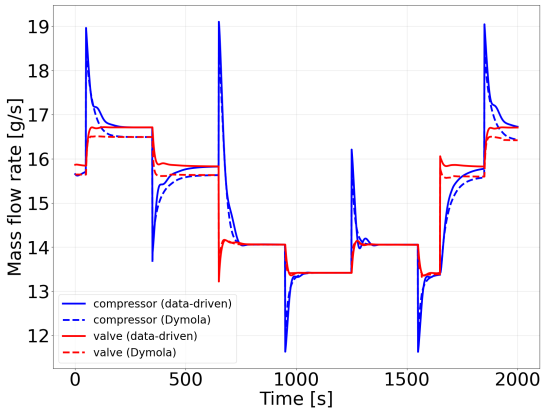

(c) Refrigerant mass flow rates.

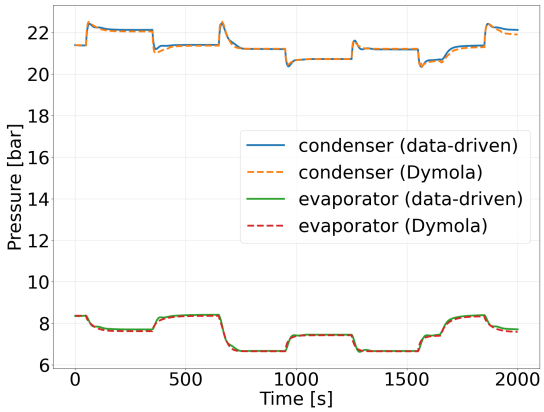

(d) HX capacities and compressor power.

Figure 6: Comparisons between data-driven models and physics-based models implemented in Dymola.

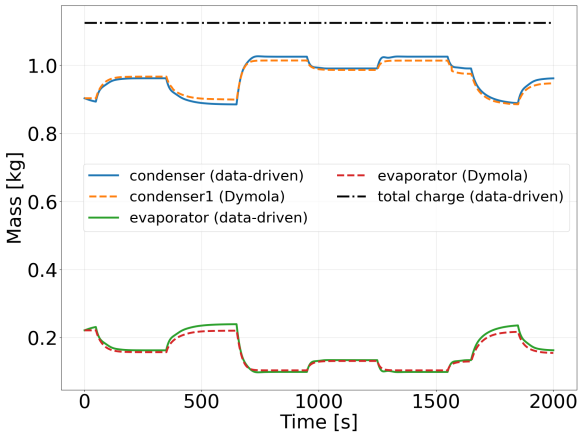

Figure 7: Refrigerant mass migration and conservation.

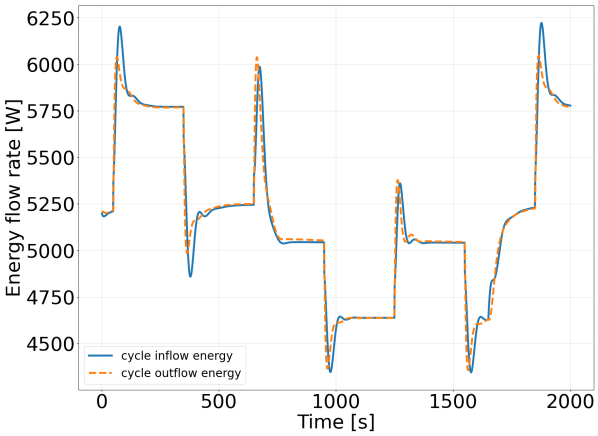

Figure 8: System energy balances

3.2 Simulation results

Component models described above are integrated into a system model to capture load-change transients of the ASHP system driven by actuation of the mass-flow devices. Figure 5 depicts pulse signals of the compressor speed and

expansion valve opening where the valve opening is controlled by a step motor with a range of 500 steps.

To examine the performance of the data-driven models, simulation results are compared with physics-based models implemented in Dymola in terms of accuracy and simulation speed. Figure 6 reveals results for the refrigerant pressures at HX inlets, air exit temperatures, liquid refrigerant mass flow rates, HX air-side capacities and the compressor power. It can be seen from the figure that the integrated data-driven system model reproduces system responses in terms of these predicted quantities in good agreement with the physics-based model. To quantify the prediction accuracy of the data-driven model against the physics-based counterpart, mean absolute percentage error (MAPE) is computed for each predicted variable to measure discrepancies between time-series data sets

$$\text{MAPE}(\mathbf{y}_{1:n}, \hat{\mathbf{y}}_{1:n}) = \frac{1}{n}\sum_{t=1}^{n}\left|\frac{y_t - \hat{y}_t}{\hat{y}_t}\right| \times 100\% \tag{18}$$

where $\mathbf{y}_{1:n}$ represents the data-driven model predictions and $\hat{\mathbf{y}}_{1:n}$ represents those of the physics-based model in this case. The maximum MAPE value of 1.25% was obtained for the evaporator capacity predictions while MAPE values for all other predicted variables are below 1%, indicating that the data-driven system model can well capture and generalize system dynamics and achieve a similar level of accuracy as physics-based models.

As stated in Section 1, of equal importance to the prediction accuracy is physical conservation properties of the data-driven system model. Figure 7 reveals the refrigerant charge migration of each HX. To verify mass conservation in the system, the sum of refrigerant charge is shown as well. It illustrates that the total refrigerant charge is completely determined at model initializtion and remains constant thereafter, which aligns with the model setup for mass conservation. Predictions of energy flows in and out of the system are tracked and depicted in Figure 8 to verify energy balances at steady-state conditions. The cycle inflow energy consists of compressor power consumption as well as the evaporator air-side capacity. Likewise, the cycle outflow energy includes the condenser capacity and the compressor heat loss. It is important to note that the inflow and outflow energy are not equal during transients due to system energy storage. However, they must be balanced at a steady-state condition with respect to the energy conservation law. As shown in the figure, energy flows of the system are balanced at all steady-state conditions, strongly supporting the energy conservation characteristic of the proposed modeling framework.

To simulate the system load-change operation spanning 2000 seconds, the physics-based Modelica model completes in 80.8 seconds, while the data-driven model completes in 24.6 seconds yielding a 3.3 times speedup by the proposed modeling approach.

4. CONCLUSIONS

This paper proposed a physics-constrained data-driven modeling approach for capturing complicated heat and mass transfer behaviors of vapor compression systems. Dynamic heat exchanger models based on gated recurrent unit are developed, and coupled to mass-flow device models based on feedforward neural networks for a modular implementation of data-driven component models. A common challenge shared by data-driven modeling paradigms is the potential violation of physical conservation laws in predictions with a lack of physical constraints to enforce those principles. To tackle it, this work proposes mass and energy conserving data-driven models with generalized interfaces that ensure a consistent system charge throughout transients and energy balances at steady-state conditions for system simulations. The proposed approach is demonstrated using a case study of an air-source heat pump system under load-change transients. Simulation results reveal good agreement between the integrated data-driven system model and a high-fidelity physics-based model implemented in Modelica with a 3.3 times speedup in simulation time.

NOMENCLATURE

A	Area	[m^2]
E	Internal energy	[J]
h	Specific enthalpy	[J/kg]
$\dot{m}$	Mass flow rate	[kg/s]
M	Mass	[kg]
p	Pressure	[Pa]
P	Power	[W]

$\dot{Q}$	Heat flow rate	[W]
t	Time	[s]
T	Temperature	[K]
η	Efficiency	[-]
ρ	Density	[kg/m^3]
ω	Frequency	[Hz]
φ	Normalized valve opening or relative humidity	[-]

Subscript

a	Air
dis	Discharge
e	Refrigerant state close to exit
is	Isentropic
i	Refrigerant state close to inlet
in	Inlet
lat	Latent
out	Outlet
r	Refrigerant
suc	Suction
v	Volumetric

REFERENCES

Chen, Z., & Fu, X. (2020). Dynamic performance prediction of vehicle variable speed air conditioner based on lstm recurrent neural network. *Energy Proceedings*, *12*.

Chen, Z., Xiao, F., Shi, J., & Li, A. (2022). Dynamic model development for vehicle air conditioners based on physics-guided deep learning. *International Journal of Refrigeration*, *134*, 126–138.

Dong, Y., Qiao, H., & Laughman, C. (2024). Physically-constrained hybrid modeling for vapor compression systems. In *9th thermal and fluids engineering conference.*

Goyal, A., Staedter, M. A., & Garimella, S. (2019). A review of control methodologies for vapor compression and absorption heat pumps. *International Journal of Refrigeration*, *97*, 1–20.

Habtom, R. (1999). Modeling a refrigeration system using recurrent neural networks. In *International conference on computational intelligence* (pp. 47–52).

Hansen, D., Maddix, D. C., Alizadeh, S., Gupta, G., & Mahoney, M. W. (2023). Learning physical models that can respect conservation laws. *arXiv preprint arXiv:2302.11002*.

Kingma, D. P., & Ba, J. (2014). Adam: A method for stochastic optimization. *arXiv preprint arXiv:1412.6980*.

Kochenderfer, M. J., & Wheeler, T. A. (2019). *Algorithms for optimization*. Mit Press.

Laughman, C. R., & Qiao, H. (2018). On closure relations for dynamic vapor compression cycle models. In *Proceedings of the american modelica conference* (pp. 9–10).

Ma, J., Kim, D., & Braun, J. E. (2021). Proper orthogonal decomposition for reduced order dynamic modeling of vapor compression systems. *International Journal of Refrigeration*, *132*, 145–155.

Qiao, H., Aute, V., & Radermacher, R. (2015). Transient modeling of a flash tank vapor injection heat pump system–part i: Model development. *International journal of refrigeration*, *49*, 169–182.

Rasmussen, B. P. (2012). Dynamic modeling for vapor compression systems—part i: Literature review. *HVAC&R Research*, *18*(5), 934–955.

Rehmer, A., & Kroll, A. (2019). On using gated recurrent units for nonlinear system identification. In *2019 18th european control conference (ecc)* (pp. 2504–2509).

Shao, L.-L., Yang, L., Zhao, L.-X., & Zhang, C.-L. (2012). Hybrid steady-state modeling of a residential air-conditioner system using neural network component models. *Energy and buildings*, *50*, 189–195.

Yang, L., Zhao, L.-X., Zhang, C.-L., & Gu, B. (2009). Loss-efficiency model of single and variable-speed compressors using neural networks. *international journal of refrigeration*, *32*(6), 1423–1432.

Yoon, Y.-J., & Lee, M. H. (2010). Dynamic simulation of vapor-compression cycle using neural networks. *International Journal of Control, Automation and Systems*, *8*, 1241–1249.